Groundwater Vulnerability Analyses using Vertical Electrical Sounding and 2D Electrical Resistivity Tomography in Papalanto South-West Nigeria

¹Ishola S.A., ²Makinde V. and ²Edunjobi O.H.

¹Department of Earth Sciences, Olabisi Onabanjo University Ago-Iwoye, P.M.B 2002, Ago-Iwoye, Ogun State, Nigeria ²Department of Physics, Federal University of Agriculture Abeokuta, P.M.B 2240,

Abeokuta, Ogun State, Nigeria.

Corresponding Author: ishola.sakirudeen@oouagoiwoye.edu.ng

Abstract

Leachate in the subsurface groundwater system originating from point or non-point sources can be delineated through an integration of qualitative and quantitative methods. Vertical Electrical Sounding (VES) and 2-D Electrical Resistivity Tomography surveys using Schlumberger and Wenner arrays were respectively adopted. The basic field equipment used for the study is AGI Super Sting Earth Resistivity meter which displays apparent resistivity value digitally as computed from Ohm's law. The depth to the aquifer varies from 8.5m to 100m while the longitudinal unit conductance (S) and hence, the protective capacity (P_c) values in the study areas are generally less than 1.0 Siemens ($P_c < 1.0$ Siemens) except in few locations around VESPAP2, VESPAP4, VESPAP10, VESPAP12, VESPAP13, VESPAP20 alongside VESPAP21 and VESPAP22; they are classified as low and are characteristics of depositional successions of overburden layers with no significant impermeable clay/shale overlying rock. Such subsurface model is an indication of high infiltration rates from precipitation as well as surface contaminants into the aquifer system. However, the aforementioned investigated locations where the protective capacity values are greater than 1.0 ($P_c < 1.0$ Siemens); imply that these locations have considerable layers of Clay separating the subsurface aquiferous zones. In addition to high transmissivity and low protective capacity values in all the investigated locations of the study area, the aquifers are very close or relatively close to the surface (<100m) and thus prone or susceptible to contamination over large areas once the aquifer receives a load of contaminant dose from surface to near surface and infiltrate the subsurface with unprecedented impacts on the groundwater system. The analysis of Papalanto pseudosection portrays a thick fine-grained Shale and Clay cover of a significant thickness values overlying the Limestone and Sandstone formation which suggests a significant productive groundwater potentials and lower aquifer vulnerability potentials of the hydrogeologic unit due to the possible retardation of the contaminant seepages by the overlying less porous and permeable Shale/Clay cover. ERT and VES indicated a polluted depth of over 24m beneath the subsurface which coincides with the upper section of the second aquifer in the study area and serves as an indication for a possible impairment of the first groundwater harness by majority of the inhabitants through shallow wells.

Keywords: Leachate, Vulnerability, Resistivity Tomography, Protective capacity, Borehole, Water Quality

INTRODUCTION

The significance of quantitative and qualitative groundwater sources to most forms of life cannot be overemphasized. Groundwater provides potable water to an estimated 1.5 billion people worldwide daily [DFID, 2001], serves as basic sustenance to other forms of biological population which includes forest plants, arable plants, ornamental plants, and livestock (Ishola et al., 2019). It has been proven to be the most reliable resource for meeting rural water demand in sub-Saharan Africa [MacDonald and Davies, 2000]. Boreholes equipped with hand-pumps are a common technology adopted by poor rural communities, and there are currently well over 250,000 hand-pumps in Africa [HMT, 2003]. In 1994, it was estimated that 40-50% of hand-pumps in sub- Saharan Africa were not working [BIDR, 1994; Bello et al., 2013]. This is backed up by more recent data from Uganda [DWD, 2002] and South Africa [Hazelton, 2000], which indicated similar operational failure rates. An evaluation in Mali in 1997 found 90% of pumps inoperable just one year after installation [World Bank, 1997]. The primary reason for these high failure rates, and hence low sustainability, is insufficient attention to operation and maintenance of the pump [Harvey and Reed, 2004]. This borehole itself, however, is sometimes the source of the problem. The quality of water for drinking deteriorates due to inadequacy of treatment plants, direct discharge of untreated sewage into rivers and stream, and inefficient management of piped water distribution system (UNEP, 2001; Ajayi and Adejumo, 2011). The contaminated water therefore has critical impact on all biotic components of the ecosystem, and this

could affect its use for other purposes. Each year about two million people die as a result of poor sanitation and contaminated water, ninety percents (90%) of the victims are children [Anon, 2009]. These hazardous effects emanate from the presence of toxic elements of environmental concern in groundwater system; elements such like Pb, Cd, As and Cr. Many of these metals have been found to act as biological poisons even at low concentration (parts of per billion ppb) levels [Okoronkwo, et al., 2005]. Bairds, 1995 also observed that the elements are toxic in the form of cations and when bonded to short chains of carbon atoms may not be toxic as free elements. Even most celebrated metals with important commercial uses are also not left out and undesirable for indiscriminate hence release into the environment [Bunce, 1990]. This research work aims to showcase the effectiveness of hydrogeophysical method in groundwater quality assessment of Papalanto communities [Ishola, 2019; Ishola et al., 2021]. The Hydrogeophysical methods utilized are electrical resistivity tomography ERT, and vertical electrical sounding **VES** methods. Electrical Resistivity Tomography (ERT) is technique for imaging the subsurface electrical structure using electrical currents. From a series of electrodes, low frequency electrical current is injected into the subsurface, and the resulting potential distribution is measured (Ayolabi et al., 2013). Early development of ERT in geophysics was confined to imaging rock core samples in the laboratory [Daily et al., but prototype data-collection 1987], hardware and research-grade inverse codes suitable for field scale applications soon followed [Daily et al., 1987; Ayolabi et al., 2013]. The method has been developed to

detect leaks from large storage tanks [Ramirez et al., 1996], monitor underground air sparging [LaBrecque et al., mapping and movement contaminant plumes [Daily et al., 1998]. More recently, ERT has been used for locating shallow cavities, fractures, fissures and mapping groundwater flow [Auken et al., 2006], identification of geological structures [Al-Sayed and El-Qady, 2007], engineering and environmental surveys [Pellerin, 2002; Olorunfemi et al., 2004; Corriols and Dahlin, 2008; Nigm et al., 2008; Ayolabi et al., 2009; Ayolabi et al., 2010; Ishola et al., 2021], and in agriculture [Giovanni, 2010]. Unsanitary particularly has devastating effects on young children in the developing world. Each year, more than 2 million persons, mostly children less than 5 years of age, die of diarrheal disease [Kosek et al., 2000]. For children in this age group, diarrheal disease accounted for 17% of all death from 2000 to 2003 ranking third among causes of death, after neonatal causes and acute respiratory infections [WHO, 2005]. Nearly 90% of diarrheal-related deaths have been attributed to unsafe or inadequate water supplies and sanitation conditions affecting a large part of the world's population [Hughes and Koplan, 2005; WHO, 2004]. An estimated 1.1 billion persons (one sixth of the world's population) lack access to clean water and 2.6 billion to adequate sanitation [Hughes and Koplan, 2005; WHO, 2005]. The principal objectives of municipal water are the production and the distribution of safe water that is fit for human consumption [Umeh et al., 2005; Lamihanra, 1999]. Over the years in Nigeria, drinking water is commercially available in easy-to-open 50-60ml polyethylene sacks known as sachet water [Hughes and Koplan, 2005]. Conformation

with approved standard is of special interest because of the capacity of water to spread diseases within a large population. Although the standards vary from place to place, the objective anywhere is to reduce the possibility of spreading water-borne disease in addition to being pleasant to drink, which implies that it must be wholesome and palatable in all respects [Harvey and Reed, 2004; Okonko et al., 2008; Edema et al., 2001]. Therefore, the necessity of collaborative, a interdisciplinary effort to ensure global access to safe water, basic sanitation, and improved hygiene is the foundation for ending cycle of poverty and diseases [Hughes and Koplan, 2005]. In line with objective of MDG (Millennium Development Goals) adopted by the Federal Republic of Nigeria is the provision of safe potable water and because of the limitation of funds for this provision and others, Ogun State of Nigeria adopted the provision of safe borehole water to augment that of treated water in all parts of the state including Papalanto metropolis. High level of chlorine in treated public water supply could react with organic matters to form organochlorine compounds which has been found to be carcinogenic when consumed over a long period of time. Hence, a high percentage of people are turning to the use of borehole water for domestic chores and drinking. Therefore, it should come as no surprise that in communities throughout the world, improving household water quality by point-of-use treatment reduces risks of diarrheal disease and significantly improves the qualities. The objectives of this are to investigate study vulnerability of the subsurface system to contaminant seepages and determine the physicochemical parameters of the borehole and hand-dug well water sources

utilizing the integration of hydrogeophysical and biogeochemical techniques.

Geology of the Study Area

Papalanto area is approximately bounded by longitude 3°13¹E and 6°54¹N and harbours one of the largest outcrops of Ewekoro limestone that easily attracts attention. It extends from Ibesse, 4km east of Papalanto along Papalanto-Shagamu road to Ogun River, 5km east to Iro community (WAPCO, 2001). The Ewekoro formation at the type locality is composed of 11m to 12m of limestone. It is sandy at the base grading downward into Abeokuta Formation. The Ewekoro formation is overlain of phosphatic glauconitic grey shale (Jones and Hockey, 1964; Fidelis et al., 2004; Ishola et al., 2021).

The Ewekoro formation is the local geology in the study area which is generally consistent with the regional geology of eastern part of the Dahomey Basin; predominantly comprises of the noncrystalline and highly non-fossiliferous limestone and thinly laminated fissile and probably non-fossiliferous shale (Ushie et al., 2014). It is the sedimentary terrain of southwestern Nigeria. Ewekoro formation consists of intercalations of argillaceous sediment. The rock is soft and friable but in some places cement by ferruginous and siliceous materials. The lithological units in Ewekoro formation are clayey sand, clay, shale, marl, limestone, and sandstone).

The Abeokuta formation was defined by Jones and Hockey (1964) to consist of grits, loose sands, sandstones, kaolinitic clay and shale and was further characterized as usually having a basal conglomerate or basal ferruginized sandstone (Archibong, 1978; Okosun, 1990 and Chene, 1978).

The Abeokuta formation on surface outcrops comprises mainly sand with sandstone, siltstone, silt, clay, mudstone, and shale interbeds. It usually has a basal conglomerate which may measure about 1m in thickness and usually consists of poorly rounded quartz pebbles with silicified and ferruginized sandstone matrix or a softly gritty white clay matrix. In outcrops where there is no conglomerate, a coarse, poorly sorted pebbly sandstone with abundant white clay constitutes the basal bed. The overlying sands are coarse grained clayey, micaceous, and poorly sorted and indicative of short distances of duration of transportation or short weathering and possible derivation from the granitic rocks located to the north. Subsurface data on the Abeokuta formation obtained from Ise-2, Afowo-1, Orimedu-1, Bodashe, Ileppawi, Ojo-1 and Itori boreholes by Okosun (1998). The formation has a thickness of 849m, 898m, 624m, 54.4m and 888m in Ise-2, Afowo-1, Ileppawi, Itori and Ojo-1 boreholes respectively. In the Ise-2 borehole, the essentially arenaceous sequence between 1261.5m and 2142.1m which consists of sands, grits, sandstone, siltstone, clay, and shale constitutes the formation. The interval 1076m - 1907m which is made up of very coarse loose sands with sporadic thin intercalations of multicoloured shale and limestone represents the formation in Ojo-1 borehole. The strata from the 44m to 98.4m in the Itori borehole, which consists of coarse-fine and medium-grained sand, silt, and sandy clay horizons, constitutes the upper portion of the formation. The Ise-2 borehole also penetrated basal conglomerate.

Jones and Hockey (1964) revealed Ewekoro limestone and the overlying Akinbo shale to be lateral equivalents of the Imo formation of eastern Nigeria. Other authors such as Omatshola and Adegoke (1991)and Oladeji (1992)have investigated the stratigraphy and depositional characteristics of limestone and clay/shale deposits in south- western Nigeria. The West African Portland Cement Company also conducted extensive geological survey and commercial appraisal of Ewekoro limestone and shale beds for commercial cement production (Ishola et al., 2021). Fig. 1 shows the Geological Map of the Selected Locations

of the Study Area within the Nigerian Part of Dahomey Embayment, Fig. 2 Displays the GoogleEarth imagery of the selected Investigated study area within in Ewekoro LGA, Southwest Nigeria, the map of Ogun State showing the geology of the study areas is presented in Fig. 3, the inset map showing political divisions of the study area within Nigerian continental environment is shown in Fig. 4, the maps of the investigated locations in the study area are shown in Fig. 5 (Ishola, 2019).

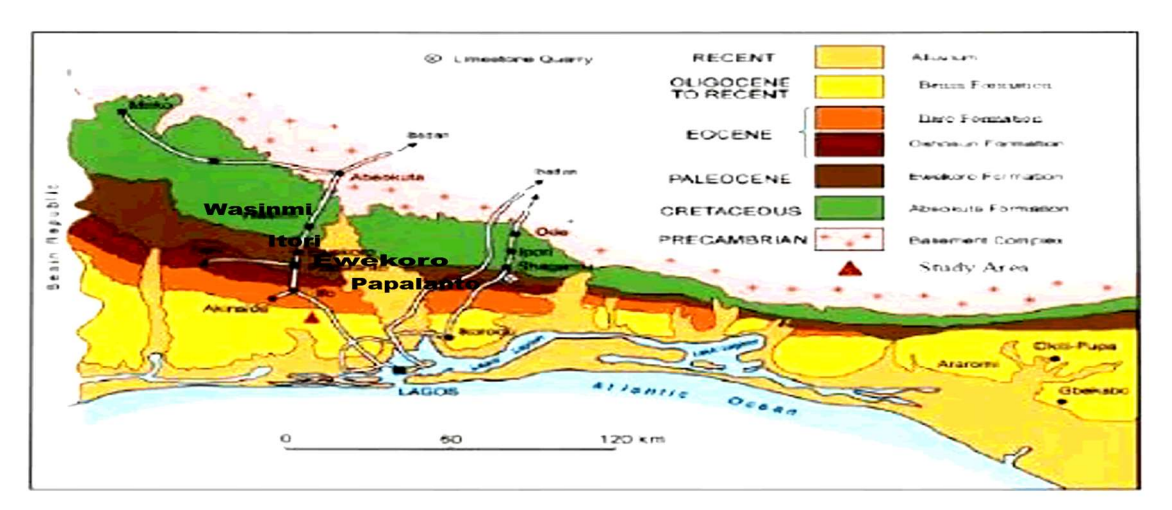


Figure 1: Geological Map Showing the Selected Locations of the Study Area within the Nigerian Part of Dahomey Embayment (Billman, 1992; Modified by Ishola, 2019).



Figure 2: Display of GoogleEarth Imagery of the selected Investigated study area within Ewekoro LGA, Southwest Nigeria (Ishola, 2019).

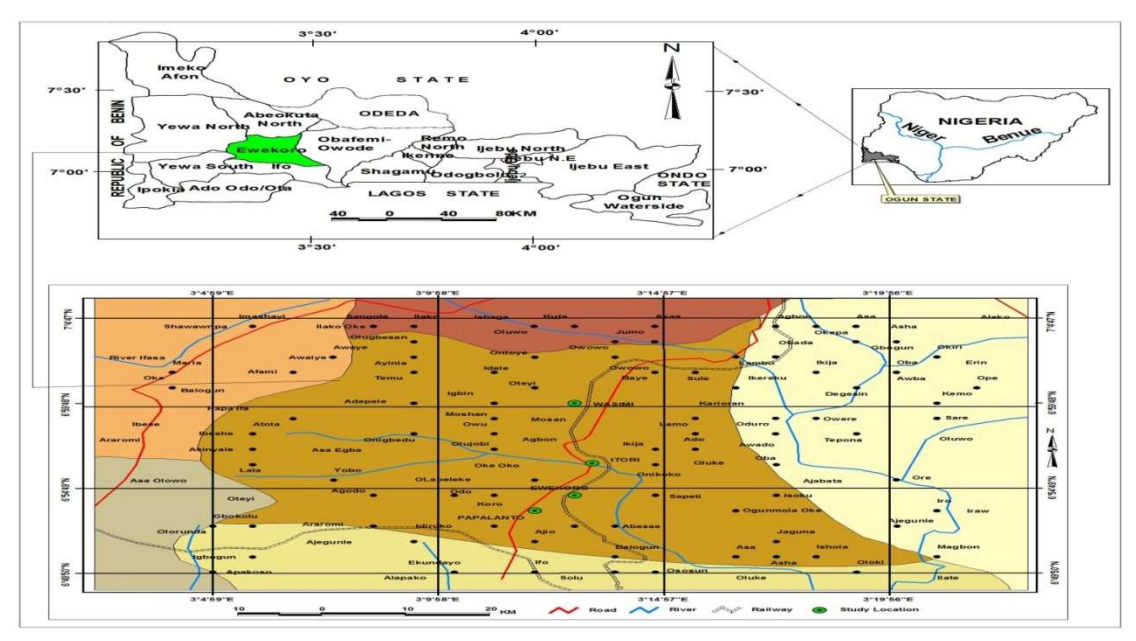


Figure 4: Inset Map showing the Study Areas in Ogun State within Nigeria Continental Domain using Esri Data/Nigeria Political Information in ArcView GIS 3.2A Environment (Ishola, 2019).

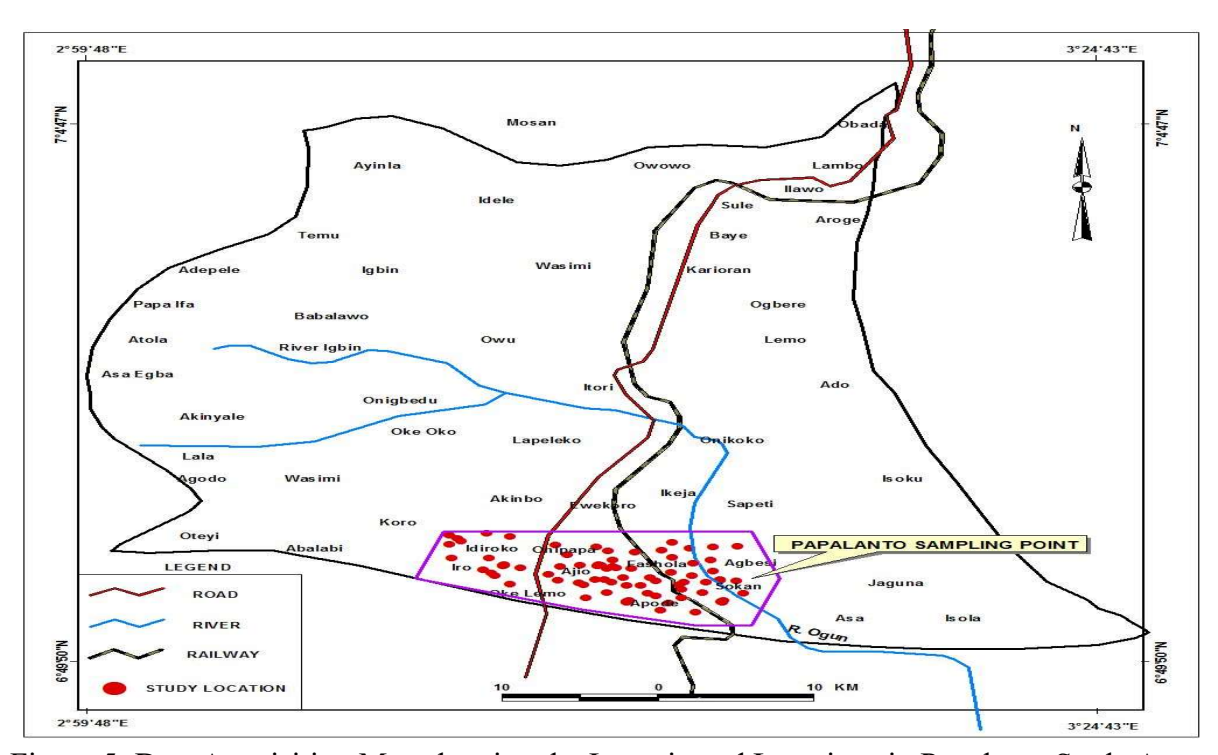


Figure 5: Data Acquisition Map showing the Investigated Locations in Papalanto Study Area in Ewekoro LGA, Southwest Nigeria (Ishola, 2019).

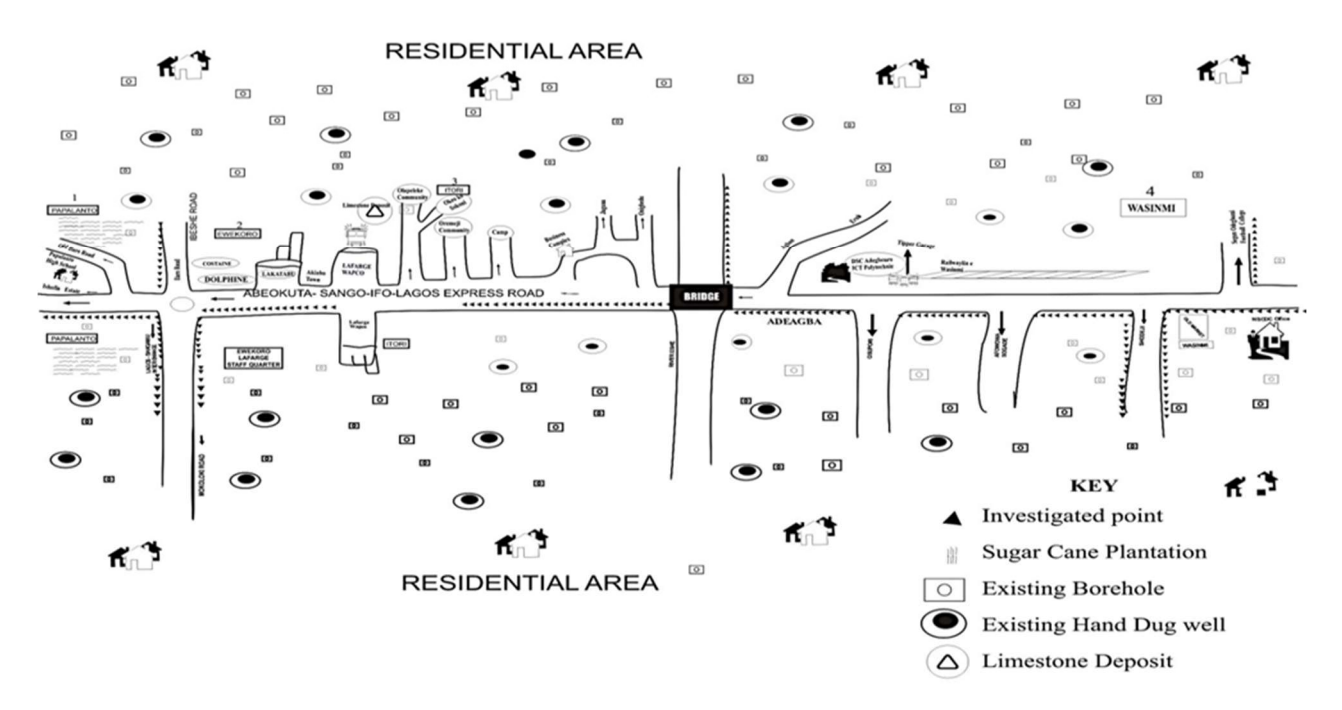


Figure 6: Basemap showing the Location and Accessibility of the Investigated Points in Ewekoro LGA, Southwest Nigeria (Ishola, 2019).

ELECTRICAL RESISTIVITY METHOD (VES AND 2D-ERT)

In this section, both Vertical Electrical Sounding (VES) and 2-D geoelectrical resistivity surveys using both Schlumberger and Wenner arrays were respectively adopted (Fig. 5a and Fig. 5b). The basic field equipment used for the study is AGI Super Sting Earth Resistivity meter which displays apparent resistivity value digitally as computed from Ohm's law. Other materials that accompany the equipment are measuring tape, 4 reels of multi-core cables, 4 hammers, 45 metal electrodes where 4 metal electrodes was used for VES and the twenty metal electrodes for 2-D. In the VES where Schlumberger configuration was adopted, the four electrodes positioned symmetrically along a straight line, the current electrodes on the outside and the potential electrodes on the inside. To change the depth range of the

measurements, the current electrodes are displaced outwards while the potential electrodes in general, are left at the same position. When the ratio of the distance between the current electrodes to that between the potential electrodes becomes too large, the potential electrodes must also be displaced outwards otherwise the potential difference becomes too small to be measured with sufficient accuracy 1979; (Koefoed, Alile, 2008). Measurements of current and potential electrode positions are marked such that $AB/2 \ge MN/2$.

Where AB/2 = Current electrode spacing and MN/2 = Potential electrode spacing

Generally, the arrangement consists of a pair of current electrodes and a pair of potential electrodes. These are driven into the earth in a straight line to make a good contact with the earth. The current electrode spacing is expanded over a range of values for measurements in the field. The values of AB/2increase as the measurements progresses while the potential electrodes separations are guided accordingly. The potential electrodes are kept at small separations relative to the current electrodes separations (Alile and Amasadun, 2008). One of the major advantages this method has over other methods is that only the current electrodes need to be shifted to new position for most readings while potential electrodes are kept constant for up to three or four readings (Dobrin, 1985; Alile, 2008). During the field work, the AGI Super Sting Earth Resistivity Meter functions as an automated resistivity meter which performs both the function of resistivity meter and a computer. As a resistivity meter it sends current into the subsurface via a pair of potential electrodes and performs automatic recording of both voltage and current, stacks the results, computes the resistance in real time which it multiplies with the

geometrical factor (a function of the distance within the current and potential electrodes) to give the resistivity and digitally displays it. As a computer the resistivity metre controls the switch box (electrode selector) on which four set of electrodes were chosen for each reading. The four set of electrodes were chosen based on the array type (Dobrin, 1985; Mamah and Eze, 1988; Alile and Amasadun, 2008). Twenty-Five (25) depth soundings were conducted, with current electrode spacing (AB) ranging from 200-340 m using Schlumberger Configuration (Fig. 7a). The 2D electrical resistivity data were acquired along 10 traverses using Wenner Array (Fig. 7b). Wenner electrode configuration was chosen for its relative sensitivity to vertical changes in the subsurface resistivity below the centre of the array and for its ability to resolve vertical changes (i.e. horizontal structures). Electrode spacing of 10 m for the profile length of 200 m was maintained to attain a reading within the depth range of aquifer in the area.

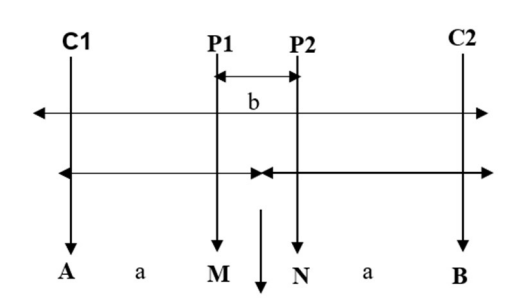


Figure 7a: Schlumberger Electrode Configuration on the Field

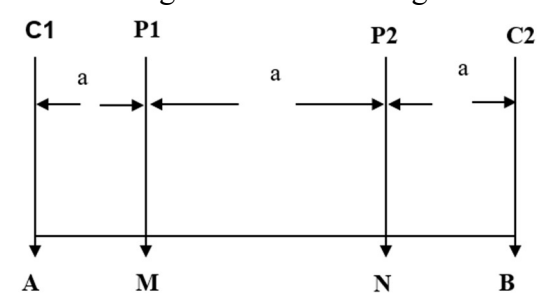


Figure 7b: Wenner Electrode Configuration on the Field

Hydrogeophysical Data Processing, Inversion, and Interpretation

The observed apparent resistivity dataset for the resistivity soundings was plotted against half-current electrode spacing (AB/2) on bi-logarithmic graph sheets. The field-curves obtained were then curvematched with Schlumberger master curves to delineate the number of layers and estimate of the corresponding resistivity and thickness of the delineated layers. The estimated geoelectric parameters were then used as initial models for computer iterative modelling on a Win-Resist program to obtain model geoelectric parameters for the delineated layers (Vander Velpen, 2004). Through an iterative process, the program varies the obtained number of layers, thickness, and electrical resistivity of each layer, until it finds a final geoelectric model that satisfactorily best fits the data. The data was downloaded from the automated system in stg. Format and can be viewed with notepad. The data was processed for bad data points such as negative resistivity before inversion was carried out. Both processing and inversion were carried out with RES2DINV software. The software plots the field or measured pseudosection and generates a calculated or theoretical model. It then carries out inversion by comparing both the measured and calculated model to generate an inverted model which is a representative of the true subsurface resistivity at different depth investigated. Similarly, the observed 2D apparent resistivity dataset for each traverse were processed and inverted concurrently using RES2DINV inversion code (Loke and Barker, 1996). The RES2DINV program uses a non-linear optimization technique that automatically determines the inverse model of the 2D

resistivity distribution of the subsurface for the measured apparent resistivity data set (Griffiths and Barker, 1993; Loke and Barker, 1996). The RES2DINV program subdivides the subsurface into a number of rectangular blocks according to the spread and density of the observed data. The size and number of the blocks is determined by survey parameters (electrode configuration, electrode separations and positions cum data level) used for the data measurements. Least-squares inversion technique with standard least-squares constraint (L₂- norm or smoothness), which minimizes the square of the difference between the observed and the computed apparent resistivity was used for the data inversion. The least-squares equation for the inversion was solved using the standard Gauss-Newton optimization technique. Smoothness constraint was applied to both data and model perturbation vectors; appropriate damping factor for inversion was selected based on the estimated noise level on the measured data. This 2D inverted section (2D Electrical Resistivity Tomography) is colour coded. The 2D ERT is provided by a colour bar scale while the horizontal and vertical scales are lateral distance and depth investigated respectively. The 2D ERT was analysed by first observing the resistivity range of the subsurface on the colour bar. resistivity distribution of subsurface was observed both vertically and laterally on the 2D ERT. The location of each traverse was noted and the electrical resistivity distribution on each 2D ERT was analysed based on the geological implication. Abrupt changes in electrical resistivity and localized anomalously high or low electrical resistivity may be due to buried non-conductive or leachate

respectively. The depth at which similar electrical resistivity distribution that may be a response from the same subsurface material was also specified during analysis (Loke, 2000; Alile, 2008; Alile et al., 2008).

RESULTS AND DISCUSSIONS

Analyses of Vulnerability Status using Vertical Electrical Sounding

Representative inverse model curves for the geoelectric parameters obtained from the computer iteration of the resistivity soundings are shown in Fig. 8. The summary of the geoelectric parameters obtained from the inverse model curves are presented in Table 1. In general, the resistivity sounding curves obtained from the surveyed area was a typical 4 layer (H type), with few 5-layer (KH). The H-type curve with about 82.4% of occurrence and KH-type curve with about 17.6% of occurrence were deduced from the area. Worthington (1977) showed that field curves often mirror image geoelectrically revealing the nature of the successive lithologic sequence in an area and hence can be used qualitatively to assess the groundwater prospects of an area. The H and KH curves which are often associated with groundwater possibilities (Omosuyi, 2010) are pertinent to the study area. The geoelectric parameters of the lithologic units were delineated from the interpreted sounding curves and shown on Table 1 since Electrical resistivity methods primarily reflect variations in ground resistivity (Omosuyi et al., 2008; Oyedele and Adevemo, 2001 and Okafor and Mamah, 2012; Aizebeokhai et al. 2010b). geoelectric parameters of the delineated layers show consistency among the sounding curves, particularly in the deeper sections where the model resistivities and thicknesses are relatively uniform (Table 1). The lithology of the delineated geoelectric layers was established by integrating available from lithologic information samples collected from boreholes and hand-dug wells, known local geology and previous (Aizebeokhai studies al.2010a: et Aizebeokhai and Oyebanjo, 2013; Aizebeokhai and Oyeyemi, 2014). The delineated geoelectric layers (from top to bottom) are characterized as top soil, sandy clay/clayey sand, shale/clay, sand lens, lateritic/kaolinitic clay, clayey sand, clay/shale, sandstone, weathered limestone and saturated sandstone. The topsoil is mainly composed of lateritic and alluvium soil and is characterized with low to high resistivity value that ranges from 9.78 – 157.23 Ωm with a mean value of 157.23±316.80. The top soil is underlain by a relatively high resistive layer that is laterally continuous across the study area; this layer is described as sandy clay/clayey sand. The large variation observed in the model resistivity of this layer is attributed to differences in the degree of compaction of the unit coupled with lateral changes in mineralogy. Underlying the second geoelectric layer is a low resistivity sandy clay or shale/clay unit observed to be laterally discontinuous in the study area while the aquiferous lithological units are karstic limestone, saturated sandstone, and sand (Ishola, 2019).

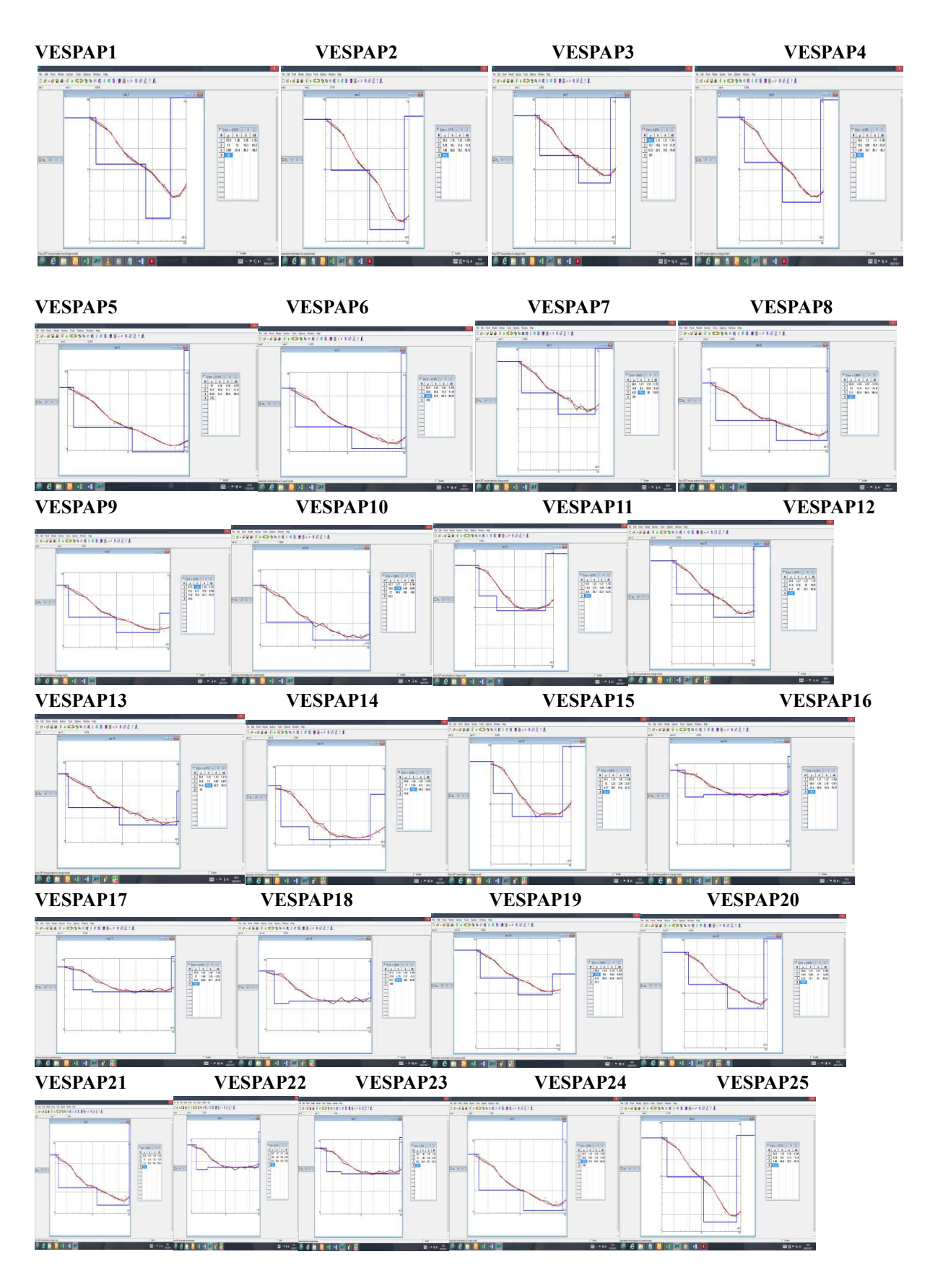


Figure 8: Cross section through VESPAP1 to VESPAP25 (Ishola, 2019)

Groundwater Levels and Protection in terms of Aquifer Types

Two general types of aquifers namely confined and unconfined aquifers are recognized. In unconfined aquifers, hydraulic heads fluctuate freely in response to changes in recharge and discharge. Water levels measured in wells completed in the upper part of an unconfined aquifer help define the elevation of the water table which is the top of the saturated zone (Ishola et al., 2016; Ishola, 2019). In confined aquifers, sometimes known as "artesian aguifers", water in the aguifers is confined under pressure by a geologic body that is much less permeable than the aquifer itself. Water levels in tightly cased wells completed in confined aquifers often rise above the elevation of the top of the aquifer. These water levels define an imaginary surface referred to as the potentiometric surface, which represents the potential height to which water will rise in wells completed in the confined aquifer. Many aquifers are intermediate between being completely unconfined or confined (Ishola, 2019).

The range and timing of seasonal waterlevel fluctuations may vary in different aquifers in the same geographical area depending on the sources of recharge to the aquifers and the physical and hydraulic properties of each. This application goes beyond standard hydrogeological applications of resistivity sounding, which commonly aim at the definition of an aguifer geometry and lithology. The combination of thickness and resistivity into single variables; the Dar-Zarrouk parameters can be used as the basis for the evaluation of properties such as aquifer transmissivity and protection of groundwater resources (Ishola, 2016). Existing boreholes located within the study areas characterized by unconfined aquifer while most are confined under pressure between relatively impermeable materials. There are great variations observed in groundwater differentiation in terms of aquifer types. The borehole locations VESPAP21 around and VESPAP23 alongside with VESPAP24 and VESPAP25 are unconfined while the rest locations displayed confined aquiferous conditions (Table 1).

Table. 1: Computed Geoelectric Parameters of Papalanto

VES Stations	Top Soil Resistivi ty (Ωm)	Dept h to Aqui fer (m)	Longitudina l Conductanc e (S)	Probable Aquifer System	Inferred Lithology	Hydraulic Conductivity (m/s)	Transmissivity (m ² s)	Protective Capacity(Slemens)
VESPAP1	52.9	46.7	0.2779927	Confined	Limestone / Sandstone	25.99945×10 ⁻³	899.57924×10 ⁻³	697.1194×10 ⁻³
VESPAP2	9.78	78	0.6681476	Confined	Limestone /Sandstone	36.07765×10 ⁻³	1284.3642×10 ⁻³	1270.718×10 ⁻³
VESPAP3	56.5	74.5	0.4145107	Confined	Limestone	25.99945×10 ⁻³	1039.9764×10 ⁻³	946.2723×10 ⁻³
VESPAP4	53.6	85.1	0.3463714	unconfined	Limestone/Sandstone	27.28436×10 ⁻³	914.02590×10 ⁻³	1221.122×10 ⁻³
VESPAP5	61	85.4	0.3475925	Confined	Limestone /Sandstone	15.15111×10 ⁻³	524.22824×10 ⁻³	972.7759×10 ⁻³
VESPAP6	62.9	84.4	0.2509664	Confined	Limestone /Sandstone	9.420362×10 ⁻³	335.36487×10 ⁻³	895.0159×10 ⁻³
VESPAP7	60.3	80	0.2174386	Confined	Limestone /Sandstone	7.114063×10 ⁻³	284.56253×10 ⁻³	920.3866×10 ⁻³
VESPAP8	65.8	96.5	0.2587825	Confined	Limestone /Sandstone	7.645165×10 ⁻³	256.11304×10 ⁻³	947.0069×10 ⁻³
VESPAP9	67.5	65.3	0.4762947	Confined	Limestone	43.78772×10 ⁻³	1532.5703×10 ⁻³	601.8433×10 ⁻³
VESPAP10	62.5	100	0.5595971	Confined	Limestone	29.44822×10 ⁻³	883.44667×10 ⁻³	1052.631×10 ⁻³
VESPAP11	53.1	62.2	0.3818059	Confined	Limestone	29.13189×10 ⁻³	1101.1855×10 ⁻³	800.4118×10^{-3}
VESPAP12	56.6	92.1	0.4767821	Confined	Limestone/ Sandstone	23.50642×10 ⁻³	655.82905×10 ⁻³	1178.201×10^{-3}
VESPAP13	70.1	92.2	0.5898912	Confined	Limestone	39.47523×10 ⁻³	1097.4115×10 ⁻³	8137.687×10 ⁻³
VESPAP14	55.8	54.6	0.4262295	Confined	Limestone	39.30507×10 ⁻³	1391.3994×10 ⁻³	646.1538×10 ⁻³
VESPAP15	51.1	61.6	0.3768276	Confined	Limestone	27.90019×10 ⁻³	1629.3710×10 ⁻³	852.2359×10 ⁻³
VESPAP16	82.8	93.4	0.3257761	Confined	Limestone /Sandstone	22.03150×10 ⁻³	586.03803×10 ⁻³	574.0627×10 ⁻³
VESPAP17	76.9	87.7	0.3431142	Confined	Limestone /Sandstone	24.90014×10 ⁻³	804.27456×10 ⁻³	590.1750×10 ⁻³
VESPAP18	67.3	100	0.4612546	Confined	Limestone / Sandstone	26.18727×10 ⁻³	785.61815×10 ⁻³	856.1643×10 ⁻³

Ishola S.A., Makinde, V. and Edunjobi, O. H.

VESPAP19	60.5	64.8	0.5839416	Confined	Limestone	45.81967×10 ⁻³	1612.8524×10 ⁻³	730.7996×10 ⁻³
VESPAP20	55.8	83	0.2308633	Confined	Limestone /Limestone	6.962047×10^{-3}	257.59575×10 ⁻³	1099.046×10 ⁻³
VESPAP21	125	38.7	0.1983077	Unconfined	Limestone+Sand	47.60194×10 ⁻³	1489.9407×10^{-3}	2172.471×10 ⁻³
VESPAP22	1428	8.5	0.7264337	Confined	Limestone+Sand	2.894540×10 ⁻³	9117.8015×10 ⁻³	4.997065×10 ⁻³
VESPAP23	36	45.14	0.2551724	Unconfined	Limestone+Sand	36.49566×10^{-3}	1273.6987×10 ⁻³	366.9919×10 ⁻³
VESPAP24	244	13.4	0.6824669	Unconfined	Limestone+Sand	30.24326×10 ⁻³	804.47081×10^{-3}	7.114774×10 ⁻³
VESPAP25	915	20.44	0.0168369	Unconfined	Limestone+Sand	38.91086×10^{-3}	762.65272×10 ⁻³	17.48502×10^{-3}

Groundwater Vulnerability in terms of Aquifer Protective Capacity

Aquifer transmissivity being defined on the hydrogeology as the product of its hydraulic conductivity for the thickness of the layer while the product of the resistivity for its thickness, it is defined as being the transverse unit resistance (T_r) , on a purely empirical basis. It can, therefore, be admitted that the transmissivity of an aquifer is directly proportional to its transverse unit resistance (Ward, 1990; Ishola, 2021). Clay layers correspond with low resistivities and low hydraulic conductivities and vice versa. Hence, the protective capacity of the overburden could be considered as being proportional to the ratio of the thickness to resistivity.

In Papalanto, all the study locations displayed less 1.0 protective capacity except VESPAP2, VESPAP4, values VESPAP10, VESPAP12, VESPAP13, VESPAP20, VESPAP21 and VESPAP22 whose protective capacities are greater than 1.0 Siemens. The highest and lowest protective capacities are found VESPAP13 and VESPAP22 respectively. The values range from 4.9971×10^{-3} Siemens to 8137.69×10⁻³ Siemens (Table 1). In the entire study locations where the longitudinal conductance (S) and hence, the protective capacity (P_c) values in the study areas are less than 1.0 Siemens ($P_c < 1.0$ Siemens); they are classified as low and are characteristics of depositional successions of overburden layers with no significant impermeable clay/shale overlying rock. Such subsurface model is an indication of high infiltration rates from precipitation as well as surface contaminants into the aquifer system. However, the investigated locations where the protective capacity

values are greater than $1.0 (P_c < 1.0)$ Siemens) imply that these locations have considerable layers of clay separating the subsurface aquiferous zones (Table 1). In addition to high transmissivity and low protective capacity values in most of the investigated locations in the study area, 92% of the aquifers are very close or relatively close to the surface (<100m) and thus prone or susceptible to contamination over large areas once the aquifer receives a load of contaminant dose from surface to near surface. Nevertheless, groundwater potential in this study areas is high due to high transverse unit resistance (R) is suitable for the development of boreholes of potable water supply (Ishola, 2019).

Analyses of Vulnerability Status using Vertical Electrical Sounding Potentials using 2D Electrical Resistivity Tomography

The 2D model resistivity of the subsurface obtained from the inversion of the observed apparent resistivity pseudosection and inverse model resistivity section are displayed in Fig. to Fig. The inverse models of the 2D resistivity of the subsurface show a general geoelectric-lithology trend very similar to that observed in the resistivity soundings. Reasonable correlation exists between the 2D inverse models and the geoelectric layered parameters obtained from the soundings. The lateral continuities of geoelectric layer (geoelectric-lithology) and near-surface heterogeneity observed in the resistivity soundings are clearly depicted in the inverted 2D resistivity images. It should be noted that the topsoil delineated in the resistivity soundings is not distinctly observed in the 2D images due to its small thickness value range of (0.5m-1.6m) averaging 1.24m in Papalanto relative to the minimum electrode spacing of 10.0m used for the 2D survey (Fig. 9a to Fig. 9e). These 2-D inverse models are used to display variation in subsurface resistivity with depth. Areas of extremely low resistivity values are attributed to leachate contamination displayed as bowl-shaped anomalous zones interpreted as contamination plume.

Geoelectric Interpretation of Subsurface Lithology along Papalanto Traverse 1 (Profile 1 and 2)

Profile 1 inverse resistivity model revealed increasing near surface resistivity values between 4.06 Ω m and 8.36 Ω m from the surface to depths of about 24.9m at a lateral distance of 15m to 200m. Profile 2 inverse resistivity model displayed a similar but more pronounced pattern of increasing near surface resistivity values ranging between 4.07 Ω m and 5.88 Ω m from the surface to depths of about 20m at a lateral distance of about 15m to 92m, 100m to 122m and 178m to 188m. This is underlain by a geologic body of lower resistivity values range of 1.95 Ω m -2.82 Ω m; this is

indicative of highly weathered and cavernous Limestone and Shale/Clay formation which serves as the underlying rock in this area (Fig. 9a).

Geoelectric Interpretation of Subsurface Lithology along Papalanto Traverse 2 (Profile 3 and 4)

Profile 3 inverse resistivity model (Fig. 9b) had resistivity values ranging from 4.60 Ω m -11.9 Ω m. The typical spread of blue portion at the base of the section shows the possible leachate conductive zone with resistivity values below 4.6Ωm which accumulated at the bottom of the section and harboured the contaminants with resistivity values ranging from 4.60 Ωm-6.03 Ω m. this therefore suggested that the plumes could have percolated rapidly into the subsurface due to the massive presence of overlying weathered and fractured rock materials of considerable thickness and depths found dominating the model and spread laterally with resistivity values ranging from 9.06 Ω m -10.4 Ω m at lateral distance of 40m to 168m.

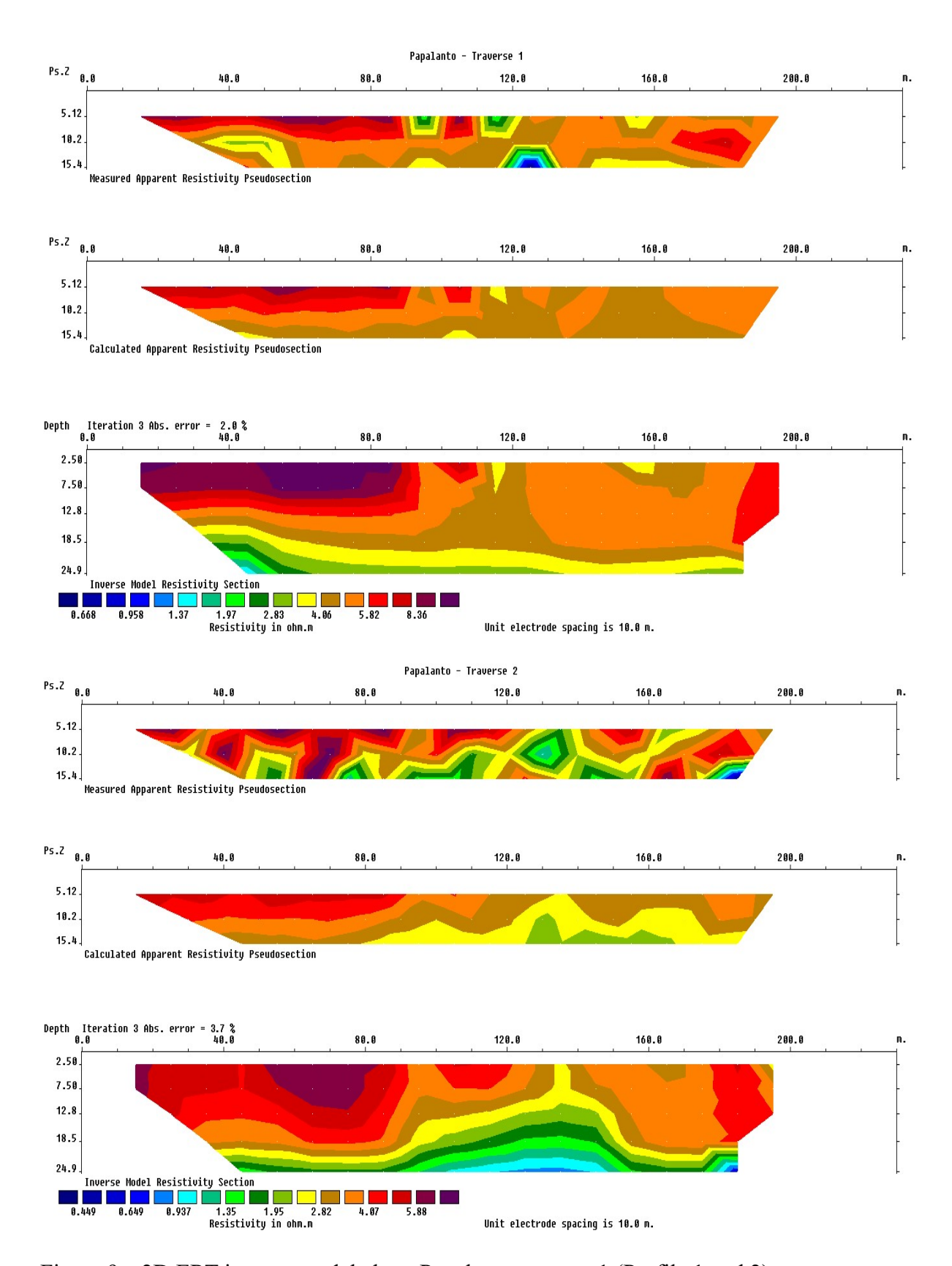


Figure 9a: 2D ERT inverse model along Papalanto traverse 1 (Profile 1 and 2)

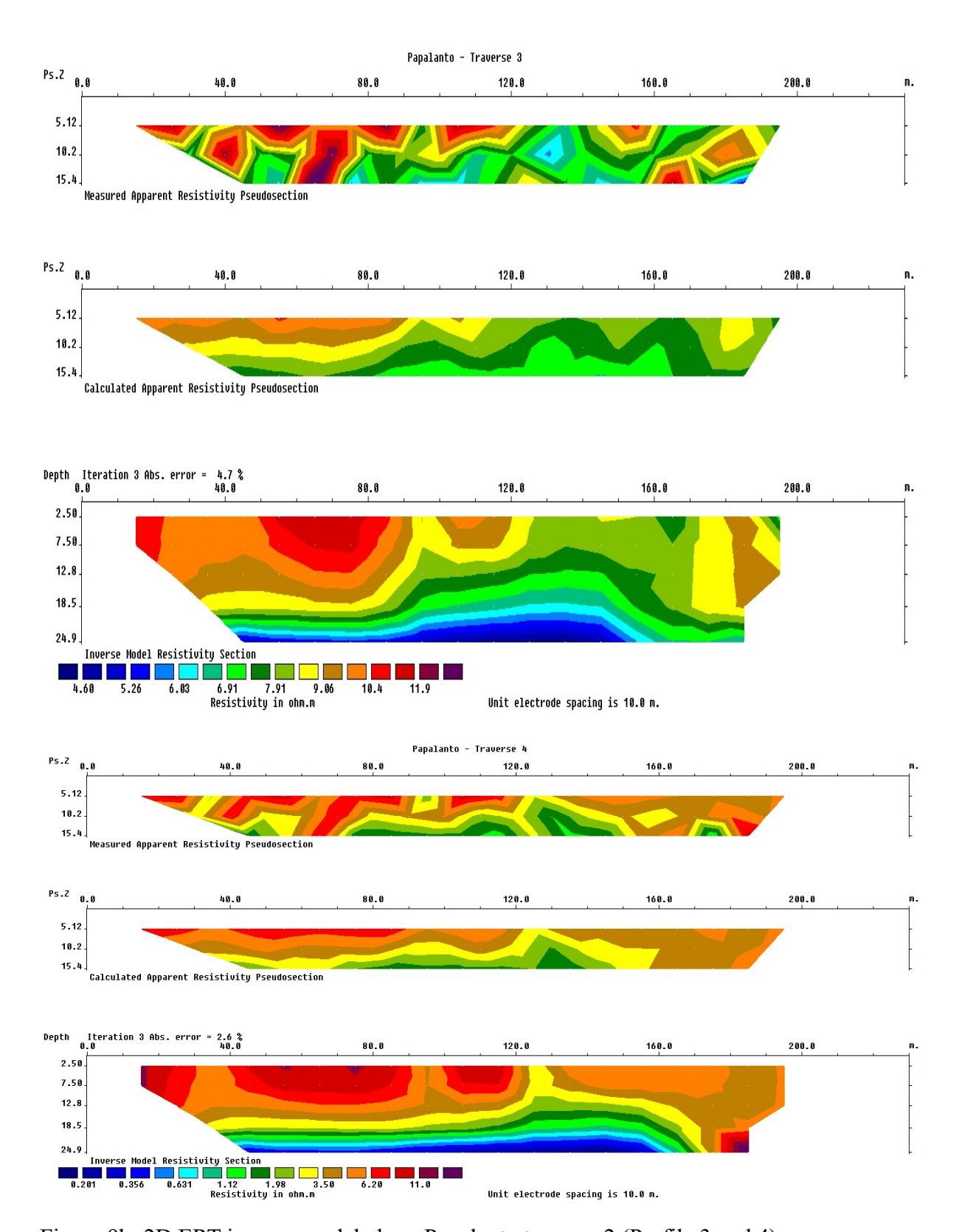


Figure 9b: 2D ERT inverse model along Papalanto traverse 2 (Profile 3 and 4)

Geoelectric Interpretation of Subsurface Lithology along Papalanto Traverse 3 (Profile 5 and 6)

Profile 5 inverse resistivity model (Fig. 9c) equally displayed electrical resistivity values ranging from $0.36\Omega m$ -12.0 Ωm . the continuous lateral spread of very low resistive geologic body at the base of the section shows the possible leachate conductive zone with resistivity values below $0.36 \Omega m$ which accumulated at the base of the section and indicated the presence of Clayey materials which harboured the contaminant seepages with resistivity values ranging from 0.36 Ωm- $0.98\Omega m$; this suggested that the possible plumes must have infiltrated rapidly into subsurface through the massive presence of weathered rock materials of considerable thickness and depth which covers and dominates about 90% of the entire model. The contaminant plumes migrate its ways vertically and laterally to the subsurface thereby leading to possible invasion of the water table of the regional aquifer system. Profile 5 inverse resistivity model (Fig. 9c) was between 7.83 Ω m and 15.7 Ω m. The distribution pattern of its contaminant plume concentrations was similar to that of Profile 5 with the exception of thicker overlying Sandy clay materials observed in Profile 6. The lateral spread of very low resistive region at the base of the section shows the possible leachate conductive zone with resistivity values below 7.83 Ω m which accumulated at the base of the section and indicate the possible presence of Clayey materials which harboured the contaminant seepages with resistivity values ranging from 7.83 Ω m -9.56 Ω m; this is an indication of that the plumes have infiltrated rapidly into the subsurface through the massive presence of weathered rock materials of lateral distances of 15m to 126m and Sandy clay formation of lateral distances of about 126m to 200m of considerable depth and thickness. These contaminant seepages thereby migrate its ways vertically and spread laterally to the subsurface leading to possible invasion of water table with unprecedented impact on the regional aquiferous zone of the study area (Fig. 9c).

Geoelectric Interpretation of Subsurface Lithology along Papalanto Traverse 4 (Profile 7 and 8)

Profile 7 inverse resistivity model showed resistivity values ranging from 4.44 Ωm -23.3 Ω m. Highly condensed zone of high conductivity was confined to depths of about 18.5m to 22m at lateral distances of 112m to 160m. This conductive region dispersed its contaminant seepages horizontally towards the base of the model and spreads uniformly and continuously at the base of the model at profile distances of about 35m to 200m. On this study area, leachates had greatly migrated to greater depths until it merges at 24.9m as shown. Profile 8 inverse resistivity model) revealed resistivity values ranging 3.40Ωm -22.4 Ω m very much similar to Profile 7. The resistivity values in this section decreases with depth (Fig. 9d).

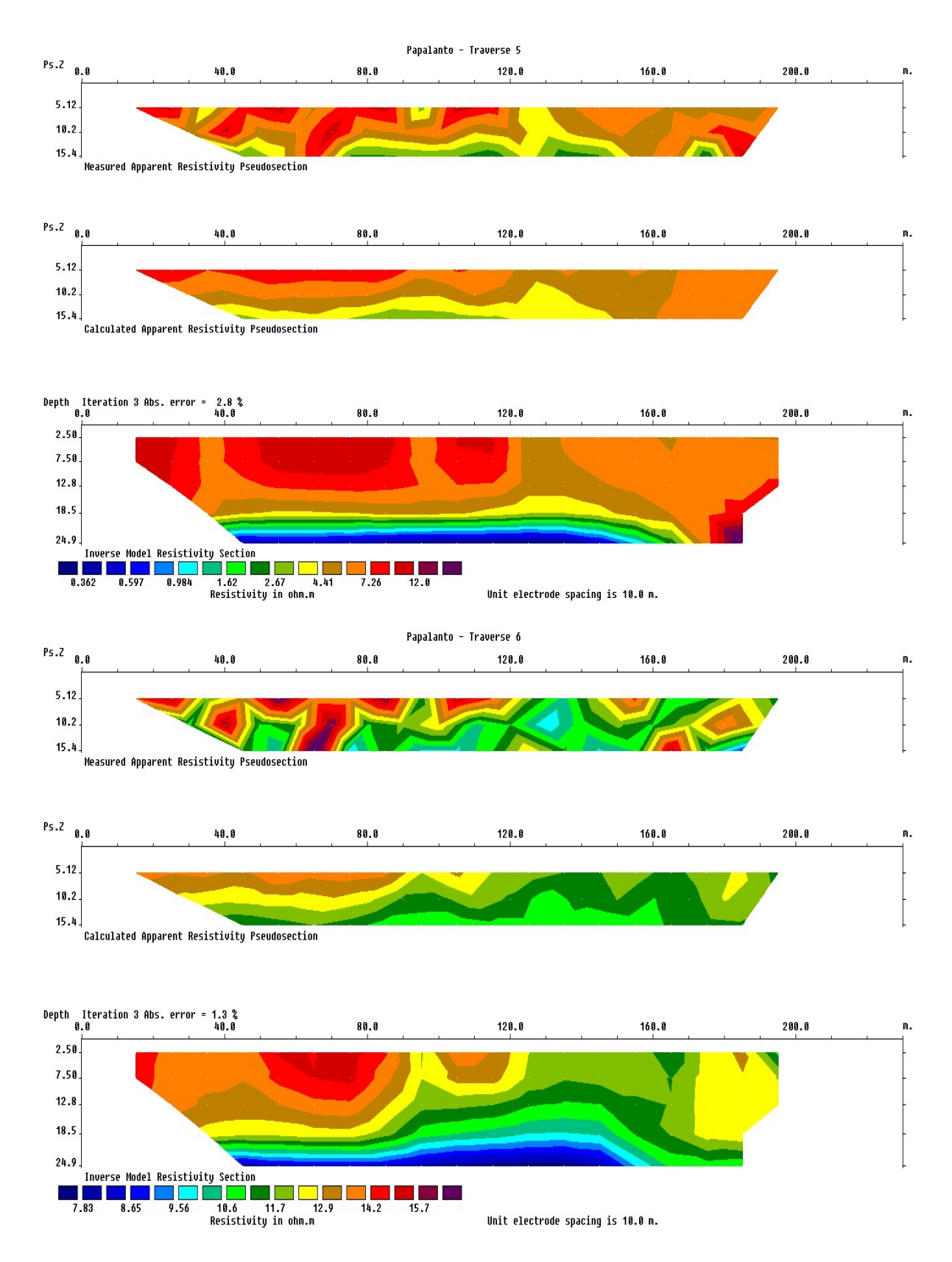


Figure 9c: 2D ERT inverse model along Papalanto traverse 3 (Profile 5 and 6)

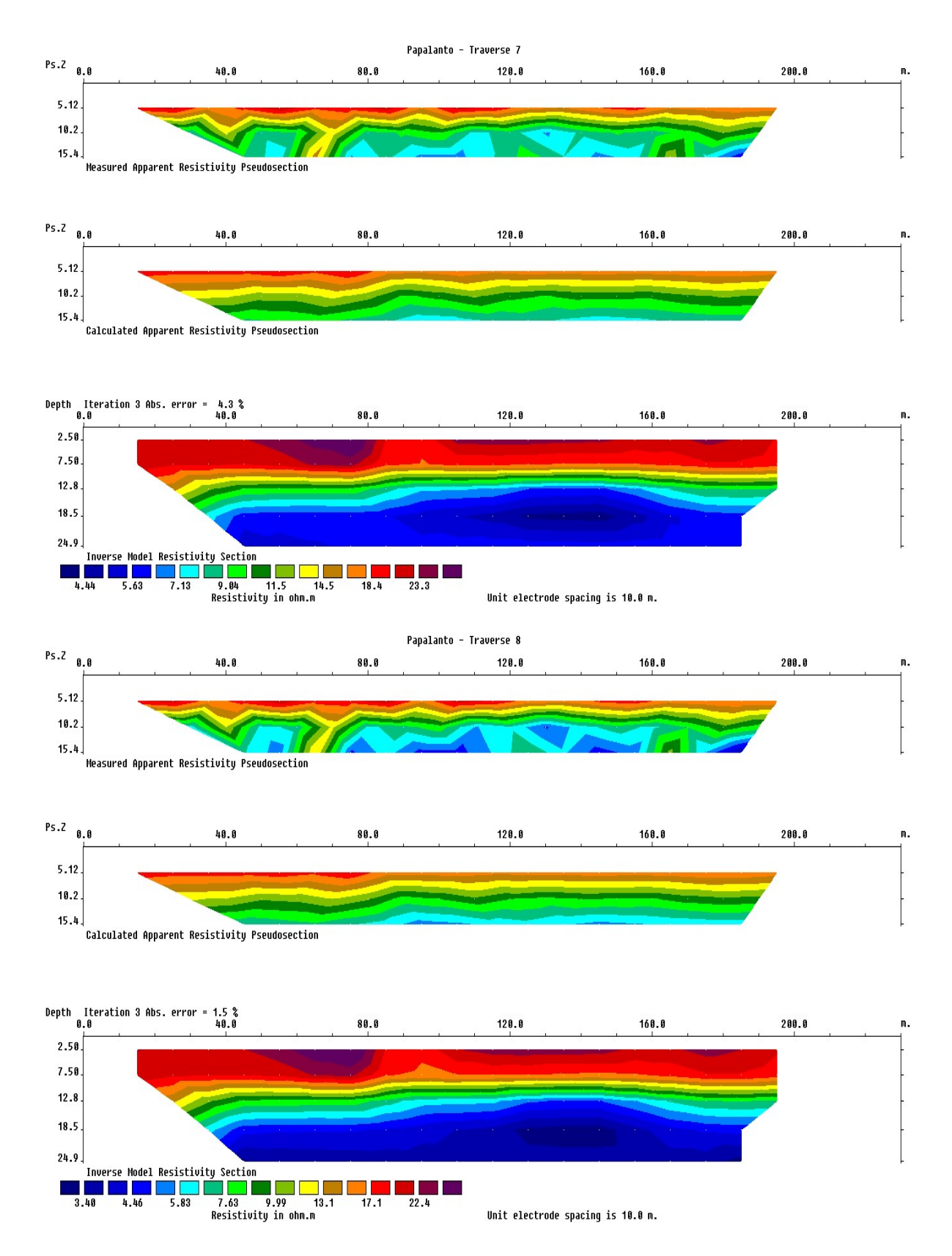


Figure 9d: 2D ERT inverse model along Papalanto traverse 4 (Profile 7 and 8)

Geoelectric Interpretation of Subsurface Lithology along Papalanto Traverse 5 (Profile 9 and 10)

Profile 9 inverse resistivity model (Fig. 9e) displayed a very low resistivity value range of $0.3~\Omega m$ - $10.3~\Omega m$ measuring from the surface of the model with the lower resistivity beneath. The lowest resistivity region spreads uniformly and continuously at the base of the section. This was regarded as conductive zone with little or no possible contaminant influence. These conductive zones were indications of the presence of clayey materials mixed with alluvium sand while the overlying rock formation of considerable thickness and depths is typically Shale.

Profile 9 inverse resistivity model had its highly conductive zone at the base of the model which spreads laterally from the centre towards the first half of both ends. It is encountered at depths of 19m and spreads laterally and continuously until it merges with depth of 24.9m. Overlying the conductive zone is Sandy clay materials and weathered Limestone formation. There is no evidence of the presence of contaminant plumes in this area but possibly due to the structural disposition of its lithology, the aquifer system of the study area is prone to contaminant seepages from the conductive zone due to the possible rapid migration of contaminant seepages through the overlying weathered rock of lateral extension of about 15m to 200m while the conductive zone spreads laterally at approximated distances of 4m to 145m (Fig. 9e).

The implication of the results of Hydrogeological Characterization of Aquifer lithological Potentials in terms of Vulnerability studies using 2D inverse resistivity model is that in most of the surveyed area, the geologic formation overlying the aquiferous zones are characterized by conductive bodies which aid the infiltrations or seepages of contaminant loads which makes them to travel down at a faster rate as they go into the aquifer storage with relative ease and enhances the migrations even within the regional aquiferous system over a large area in a relatively shorter period of time with unprecedented impact on the general groundwater quality over time.

Clayey geoelectric layers in the study area are located farther from the aquiferous zone and are mixed variably with coarse- and fine-grained alluvium sands thereby making the soil and aquifers of the study vulnerable be to leachate contamination at shallow levels. Since we interpreted the topsoil as being lateritic soils and alluvium in very few places with less clayey content, leachate infiltration in the study area is enhanced by the lack of protective layers as shown by the correlation between longitudinal conductance and overburden protective capacity. The topsoil in the study area is porous and permeable and is therefore conduits for leachate. Hence, the soils and groundwater resources around investigated locations of the study area might be polluted by possible contaminant seepages from different environmental sources. This necessitates the use of direct geochemical analyses to prove the toxicity of the existing groundwater of the area in form of boreholes and hand-dug wells based concentration level. hypothesize that with time the leachate contamination may contribute to pollution of the groundwater, and this is of great threat to domestic usage, farming, and

future exploitation of underground water resources in the study area.

Profile 10 has a higher resistivity value range of 21.9 Ω m - 37.3 Ω m and spreads non-uniformly at short intervals of lateral distance of 44m to 78m and 100m to 124m and exhibits varying thickness value of 4m to 5m; the layer is inferred to be Clay.

The third geoelectric layer is composed of Shale/Clay. It is uniformly spread through the survey length and intrudes the second layer at the lateral distance of about 33m to 153m and 167m to 200m with the thickness of 6m to 7m in Profile 9 while a resistivity value range of 12.8 Ω m - 21.9 Ω m with a non-uniform and non-continuous distribution at the lateral interval of about 19m to 45m, 78m to 100m and 123m to 200m encountered in Profile 10.

The fourth geoelectric layer is composed of Limestone with an electrical resistivity value range of 1.40 Ω m -2.30 Ω m uniformly and continuously spread beneath the third layer at a lateral distance of about 24m to 200m in Profile 9 (Fig. 4.8.5) while a higher resistivity value range of 4.40 Ω m - 7.15 Ω m is encountered in Profile 10

having a thicker layer than Profile 9. It is thicker in the NW and SE section than the central or middle location of the surveyed area of Profile 10.

Directly underlying this formation is a very low resistivity layer of values $0.89 \Omega m$ to $2.58 \Omega m$ uniformly and continuously distributed at a lateral distance of about 35m to 185m encountered at the depth of 23m in Profile 9 while a similar resistivity value range of whose intervals of spread is about 35m to 160m in lateral extent is encountered at the depth of 19m; this layer is suggestive of Sandstone with Alluvium sand materials though the actual depth and thickness could not be determined due to current termination.

The analysis of Papalanto pseudosection portrays a thick fine-grained Shale and Clay cover of a significant thickness values overlying the Limestone and Sandstone formation which suggests a significant productive groundwater potentials and lower aquifer vulnerability potentials of the hydrogeologic unit due to the possible retardation of the contaminant seepages by the overlying less porous and permeable Shale/Clay cover.

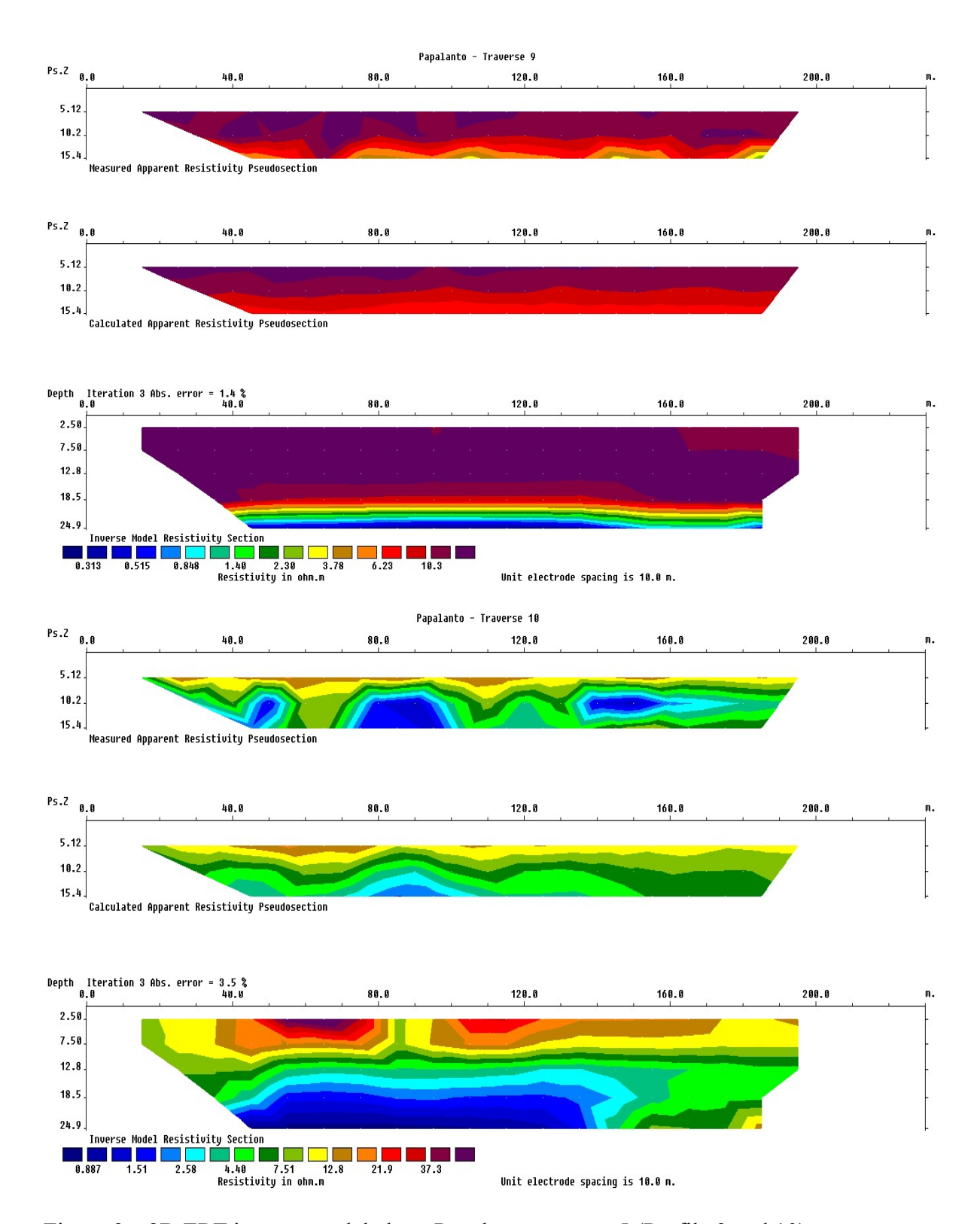


Figure 9e: 2D ERT inverse model along Papalanto traverse 5 (Profile 9 and 10)

CONCLUSION

The integrated methods have proven to be effective tools for groundwater quality assessment. The protective capacity (P_c) values in the study areas are less than 1.0 Siemens (P_c < 1.0 Siemens); subsurface model is an indication of high infiltration rates from precipitation as well as surface contaminants into the aquifer system. However, the investigated locations where the protective capacity values are greater than 1.0 ($P_c < 1.0$ Siemens) imply that these locations have considerable layers of clay separating the subsurface aguiferous zones (Table 1). In addition to high transmissivity and low protective capacity values in most of the investigated locations in the study area, 92% of the aquifers are very close or relatively close to the surface (<100m) and thus prone or susceptible to contamination over large areas once the aquifer receives a load of contaminant dose from surface to near surface. Nevertheless, groundwater potential in this study areas is high due to high transverse unit resistance (R) is suitable for the development of boreholes of potable water supply. ERT and VES indicated a polluted depth of over 24m beneath the subsurface which coincides with the upper section of the second aquifer in the study area which serves as an indication for a possible impairment of the first groundwater harness by majority of the inhabitants through shallow wells.

REFERENCES

Aizebeokhai A. P, Alile O. M, Kayode J. S, Okonkwo F. C. (2010a). Geophysical investigation of some flood prone areas in Ota, southwestern Nigeria. Am-Eurasian J Sci Res 5(4):216–229.

- Aizebeokhai A. P, Olayinka A. I, Singh V. S. (2010b). Application of 2D and 3D geoelectrical resistivity imaging for engineering site investigation in a crystalline basement terrain, southwestern Nigeria. Environ Earth Sci 61(7):1481–1492. doi:10.1007/s12665-010-0474.
- Aizebeokhai AP, Oyebanjo OA (2013)
 Application of vertical electrical soundings to characterize aquifer potential in Ota, Southwestern Nigeria. Int J Phys Sci 8(46):2077–2085
- Aizebeokhai, A.P, Oyeyemi, K.D. (2014). The use of multiple-gradient array for geo-electrical resistivity and induced polarization imaging. J. Appl Geophys 111:364–376. doi:10.1016/j.jappgeo.2014.10.02
- Ajayi, A. O. and Adejumo, T. O. (2011). Microbiological assessment and some physico-chemical properties of water sources in Akungba-Akoko, Nigeria Journal Toxicology and Environmental Health Sciences Vol. 3(13), pp. 342-346, 14 November 2011 http://www.academicjournals.org/ **JTEHS** DOI: 10.5897/JTEHS11.068 **ISSN** 2006-9820 ©2011
- Al-Sayed, E. A. and El-Qady, G. (2007). "Evaluation of Sea Water Intrusion Using the Electrical Resistivity and Transient Electromagnetic Survey: Case Study at Fan of W

- Feiran, Sinai, Egypt," EGM International Workshop Innovation in EM, Gravity, and Magnetic Methods: A New Perspective for Exploration Capri, Capri, 15-18 April 2007.
- Alile, O. M. and Amadasun, C.V.O (2008).

 Direct Current pobing of the subsurface Earth for Water Bearing Layer in Oredo Local Government Area, Edo State, Nigeria. Nigeria Journal of Applied Science, Vol. 25: 107-116.
- Alile, M. O., Jegede, S. I and Ehigiator, O. M. (2008). "Underground Water Exploration using Electrical Resistivity Method in Edo State, Nigeria". Asian Journal of Earth Sciences. 1:38-43.
- Auken, E., Pellerin, L., Christensen, N. B. and Sorensen, K. (2006) "A Survey of Current Trends in Near-Surface Electrical and Electromagnetic Methods," Geophysics, Vol. 71, No. adi 1023/A:10150442005675, 2006, pp. G249-G260.
- Ayolabi, E. A., Folorunso, A. F., Adeoti, L. Matthew, S., and E. Atakpo, S. (2009). "2-D and 3-D Electrical Resistivity Tomography and Its Implications," The 4th Annual Research Conference and Fair held at the University of Lagos, Akoka, 8 Jannuary 2009, p. 189.
- Ayolabi, E. A., Folorunso, A. F., and Obende, P. W. (2010). "Integrated Assessments of Possible Effects of Hydrocarbon and Salt Water

- Intrusion on the Groundwater of Iganmu Area of Lagos Metropolis, SW Nigeria," Earth Sciences Research Journal, Vol. 14, No.1, pp. 100-110.
- Ayolabi, E.A, Folorunso, A. F., and Kayode, O.T. (2013).Integrated Geophysical and Geochemical Methods for Environmental of Municipal Assessment Dumpsite System, International Journal of Geosciences, 2013, 4, 850-862 http://dx.doi.org/10.4236/ijg.2013 .45079: July 2013 (http://www.scirp.org/journal/ijg).
- Bairds, C. (1995). "Environmental Chemistry," W.H. Free-man and Company, New York, 1995, pp. 384-387.
- BIDR. 1994. Consult Diwi. and Bureau d'Ingénierie pour le Développement Rural (BIDR). Etudes d'Réhabilitation des Points d'Eau Existants. 1994, 11-13
- Billman, H.G. (1992). Offshore stratigraphy and paleontology of the Dahomey (Benin) Embayment, West Africa, 1st. NAPE Bull. No. 2, Vol. 7, pp. 121 130.
- Bunce, N. J. (1990). "Environmental Chemistry," Winers Publishing Ltd., Winnipeg, 1990.
- Charles, J. T and William, M. A. (2001).

 Groundwater Level Monitoring and the Importance of Long-Term Water Level Data, U.S. Geological Survey Circular 1217, Denver

Colorado, Gb1015.T282001551.4920973-Dc2.

- Chene J. (1978). Biostratigraphical study of the borehole ojo -1 south west Nigeria. Rene de micropal 21: 123-139.
- Corriols, M. and Dahlin, T. (2008). "Geophysical Characterization of the Leon-Chinandega Aquifer Nicaragua," Hydrogeological Journal, Vol. 16, No. 2, 2008, pp. 349-361.
- Daily, W. D., Lin, W. and Buscheck, T. (1987). "Hydrological Properties of Topopah Spring Tuff: Laboratory Measurements, journal of Geophysical Research, Vol. 92, No" B8, 1987, pp. 7854-7864. doi:10.1029/JB092iB08p07854
- DFID. 2001. Addressing the Water Crisis: Healthier and more productive lives for poor people, Strategies for achieving the international development targets. Department for International Development: UK., 2001,2 3.
- DWD. 2002. Overview of the Water Sector, Reform, SWAP and Financial Issues. Directorate of Wat. Dev., Ministry of Water, Lands and Environment, the Rep. of Uganda. 1(1), 2002, 12-15.
- Edema, M.O. Omemu., A.M. and Fapetu., O.M. 2001. Microbiology and Physiochemical Analysis of different sources of drinking water in Abeokuta. Nigeria. Nigerian

- Journal of Microbiology, 15(1): 57-61.
- Fidelis U., Thomas H. and Uduak A. (2014).

 Reserve Estimation from
 Geoelectrical Sounding of the
 Ewekoro Limestone at Papalanto,
 Ogun State, Nigeria. Journal of
 Energy Technologies and Policy.
 ISSN 2225-0573, www.iiste.org
 Vol.4, No.5, 2014, pp 28-33
- Giovanni, L. 2010. "The Use of Geophysical Methods for 3-D Images of Total Root Volume of Soil in Urban Environments," Exploration Geophysics, Vol. 41, No. 4, 2010, pp. 268-278. doi:10.1071/EG09034.
- Griffiths, D.H. and Barker, R.D. (1993).

 Two-dimensional resistivity
 imaging and modelling in areas of
 complex geology. J Appl Geophys
 29:211–226.
- Handzel. T. 2008. The Effect of Improved Drinking Water Quality on the Risk of Diarrheal Disease in an Urban Slum of Dhaka, Bangladesh: A Home Chlorination Intervention Trial. Doctoral Dissertation. Department of Environmental Sciences and Engineering. University of North Carolina, Chapel Hill, 2008, UNC: 110-104.
- Harvey, P.A. and Reed, R.A. 2004. Rural Water Supply in Africa: Building blocks for hand pump sustainability. WEDC, Loughborough University, UK., 2004, 46-49.

- Hazelton, D. 2000. The development of community water systems using deep and shallow well handpumps.

 WRC Report No, TT132/00,
 Water Research Centre, South Africa, 2000, 22-24.
- HTN. 2003. Focus on Africa, a critical need.

 Network for Cost-Effective
 Technologies in Water Supply and
 Sanitation, St. Gallien,
 Switzerland, 2003, 15-19.
- Hughes., J.M. and Koplan., J.P. 2005. Saving Lives through Global Safe Water. Journal of Emerging Infectious Diseases, 11(10), 2005,1636-1637.
- Ishola S.A (2019). Characterization of Groundwater Resource Potentials using Integrated Techniques in Selected Communities within Ewekoro Local Government Area South-West Nigeria. Department of Physics, FUNAAB Ph.D. Thesis.
- Jones H.A, Hockey R.D (1964). The Geology of Parts of Southwestern Nigeria. Geol Survey Nig. Bull. 31: 22 24.
- Kehinde-Phillips, T. Ogun State maps, In: Onakomaya, S.O., K. Oyesiku and Jegede, (1992). Ogun State in Maps. Rex Charles Publishers, Ibadan, pp: 187. pp187, 1992.
- Kosek., M. Bern., C. and Guerrant., R.L. 2003. The global burden of diarrhoeal disease, as estimated from studies published between 1992 and 2000. Bulletin of World Health Organization, 81, 2003,197-204.

- LaBrecque, D. J., Ramirez, A. Daily, W. and Binley. A. (1996)."ERT Monitoring of Environmental Remediation Processes," Measurement Science and Technology, Vol. 7, No. 3, 1996, pp. 375-383. doi:10.1088/0957-0233/7/3/019.
- Lamikanra. A. 1999. Essential Microbiology for students and practitioner of Pharmacy, Medicine, and Microbiology (2nd edn. Amkra books, Lagos, 1999).
- Loke, M. H, and Barker, R. D. (1996).

 Practical techniques for 3D resistivity surveys and data inversion. Geophys Prospect 44:499–524.
- Loke, M.H. (2000). RES2DINV ver.3.50.
 Rapid 2D resistivity and IP inversion using the Least Square Method. Geotomo software, Penang, Malaysia.
- MacDonald, A.M. and Davies, J. A. 2000.

 Brief Review of Groundwater for Rural Water Supply in Sub-Saharan Africa. British Geological Survey Technical Report WC/00/33, Nottingham, UK. 2000, 9-10.
- Nigm, A. A. Elterb, R. A. Nasr, F. E. and Thobaity, (2008).Η. M. "Contribution of Ground Magnetic Resistivity and Methods Groundwater Assessment in Wadi Bany Omair. Holy Makkah Area, Saudi Arabia," Egyptian. Geophysical Society Journal, Vol. 6, No. 1, pp. 67-79.

- Okonko., I.O. Ogunjobi., A.A. Adejoye., A.D. Ogunnusi., T.A. Olasogba., M.C. Comparative studies and microbial risk assessment of different water samples used for processing frozen sea foods in Ijora-olopa, Lagos State, Nigeria. African Journal of Biotechnology, 7 (16), 2008, 2902-2907.
- Okoronkwo, N. Igwe, J. C. and Onwuchekwa, E. C. (2005). "Risk and Health Implications of Polluted Soils for Crop Production" Afr Jour of Biotech., Vol. 4, No. 13, 2005, pp. 1521-1524.
- Okosun, E.A. 1990. A review of the cretaceous stratigraphy of the Dahomey embayment, West Africa. Cretac Res 11:17–27.
- Okosun, E.A. (1998). Review of the early Tertiary stratigraphy of southwestern Nigeria, Jour. Min., and Geol. Vol. 34, no 1, pp. 27–35.
- Oladeji B.O (1992). Environmental analysis of Ewekoro Formation at the Shagamu Quarry. Nig. J. Min. Geol., 28(1): 148–156.
- Olorunfemi, M. O., Idoringie, A. I. and Coker, A. T. (2004). "Application of the Electrical Resistivity Method in Foundation Failure Investigation: A Case Study," Global Journal of Geological Sciences, Vol. 2, No. 1, 2004, pp. 139-151.

- Omatsola, M. E, Adegoke, O. S (1981).

 Tectonic Evaluation and cretaceous stratigraphy of the
- Dahomey Basin, J. Min. Geol. 5(2): 78-83.
- Omosuyi G.O., Ojo J.S., and Olorunfemi, M.O. (2008). Geoelectric sounding to delineate shallow aquifers in the coastal plain sands of Okitipupa Area, Southwestern Nigeria. Pacific J Sci Technol 9(2):562–577Google Scholar
- Omosuyi, G.O. (2010). Geoelectric assessment of groundwater prospect and vulnerability of overburden aquifers at Idanre, Southwestern Nigeria. Ozean Journal of Applied Sciences Vol. 3. No.1. pp. 19-28.
- Omosuyi, G.O., Adegoke, A.O and Adelusi, A.O. (2008). "Interpretation of Electromagnetic and Geoelectric Sounding Data for Groundwater Resources around Obanla-Obakekere. Akure, near Southwestern Nigeria". The Pacific Journal of Science and Technology. 9(2):508-525.
- Oyedele, K. F., and A. O. Adeyemo. (2001).

 "Surface Electrical Resistivity

 Measurement in the

 Characterization of Groundwater

 Potentials of the Typical Basement

 Terrain, Northern
- Pellerin, L. (2002). "Applications of Electrical and Electromagnetic Methods for Environmental and Geotechnical Investigations," Surveys in Geophysics, Vol. 23, No. 2-3, 2002, pp. 101-132. doi:10.